

Ultrametricity and clustering of states in spin glasses: A one-dimensional view

Helmut G. Katzgraber¹ and Alexander K. Hartmann²

¹*Theoretische Physik, ETH Zürich, CH-8093 Zürich, Switzerland*

²*Institut für Physik, Universität Oldenburg, D-26111 Oldenburg, Germany*

We present results from Monte Carlo simulations to test for ultrametricity and clustering properties in spin-glass models. By using a one-dimensional Ising spin glass with random power-law interactions where the universality class of the model can be tuned by changing the power-law exponent, we find signatures of ultrametric behavior both in the mean-field and non-mean-field universality classes for large linear system sizes. Furthermore, we confirm the existence of nontrivial connected components in phase space via a clustering analysis of configurations.

PACS numbers: 75.50.Lk, 75.40.Mg, 05.50.+q, 64.60.-i

An ultrametric (UM) space [1] is a special kind of metric space in which the triangle inequality $d_{\alpha\gamma} \leq d_{\alpha\beta} + d_{\beta\gamma}$ [$d_{\alpha\beta}$ represents the distance between two points α and β] is replaced by a stronger condition where $d_{\alpha\gamma} \leq \max\{d_{\alpha\beta}, d_{\beta\gamma}\}$, i.e., the two longer distances must be equal and the states thus lie on an isosceles triangle. The concept appears in many branches of science, such as p-adic numbers, linguistics, as well as taxonomy of animal species. It is also an intrinsic property of Parisi's mean-field solution [2, 3, 4] of the Sherrington-Kirkpatrick (SK) [5] infinite-range spin glass. Hence, in general, the nature of the spin-glass state [4, 6] can be analyzed via clustering and ultrametricity-probing methods.

The nature of the spin-glass state is controversial and it is unclear if the mean-field picture (also known as RSB for “replica symmetry breaking”) [2], the droplet picture [7, 8], or an intermediate, more phenomenological scenario dubbed as TNT [9, 10] (for “trivial–nontrivial”) describes the nature of the spin-glass state best. One avenue to settle the applicability of the mean-field picture to short-range spin glasses is by testing if the phase space is UM. Unfortunately, the existence of an UM phase structure for short-range spin glasses is controversial, mainly because only small linear system sizes have been accessible so far. Recent results [11] suggest that short-range systems are not UM, whereas other opinions exist [12, 13, 14]. Thus it is of paramount importance to test if short-range spin glasses have an UM phase space.

In this work we approach the problem from a different angle: First, we use a one-dimensional (1D) Ising spin-glass with power-law interactions. The model has the advantage that large linear system sizes can be studied. Furthermore, by tuning the exponent of the power law, the universality class of the model can be tuned between a mean-field and a non-mean-field universality class. This allows us to test our analysis method on the mean-field SK model and then apply it to regions of phase space where the system is not mean-field like. We perform a clustering analysis of the data similar to the work of Hed *et al.* [11] to obtain nontrivial triangles in phase space and introduce a novel correlator which allows us to see an UM signature for low temperatures and (as expected

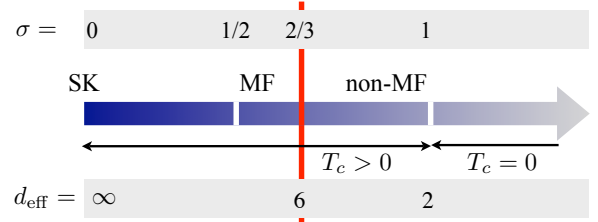


FIG. 1: (Color online) Sketch of the phase diagram of the 1D Ising chain with random power-law interactions. For $\sigma \leq 1/2$ we expect SK-like infinite-range behaviour. For $1/2 < \sigma \leq 2/3$ we have mean-field (MF) behaviour corresponding to an effective space dimension $d_{\text{eff}} \geq 6$, whereas for $2/3 < \sigma \lesssim 1$ we have a long-range (non-MF) spin glass with a finite ordering temperature T_c . Close to $\sigma = 2/3$ (vertical red line) $d_{\text{eff}} \approx 2/(2\sigma - 1)$ [4]. For $\sigma \geq 1$ $T_c = 0$.

from physical grounds) delivers no signal for high temperatures. Furthermore, we use a clustering analysis to search for connected components in phase space. Note that the proposed method can be applied to any field of science to test for an UM structure of phase space, thus making the method generally applicable.

Our results for low temperatures show that for this model the phase space has an UM signature and exhibits many phase-space components, the number growing with system size in the mean-field as well as non-mean-field case. This suggests that for large enough system sizes short-range spin glasses at low enough temperatures might have an UM phase space structure.

Model — The Hamiltonian of the 1D Ising chain with long-range power-law interactions [15, 16] is given by

$$\mathcal{H} = - \sum_{i < j} J_{ij} S_i S_j \quad J_{ij} = c(\sigma) \frac{\epsilon_{ij}}{r_{ij}^\sigma}, \quad (1)$$

where $S_i \in \{\pm 1\}$ are Ising spins and the sum ranges over all spins in the system. The L spins are placed on a ring and $r_{ij} = (L/\pi) \sin(\pi|i - j|/L)$ is the distance between the spins. ϵ_{ij} are Gaussian-distributed random couplings of zero mean and standard deviation unity. The constant $c(\sigma)$ is chosen such that the mean-field transition temperature to a spin-glass phase is $T_c^{\text{MF}} = 1$ [16].

TABLE I: Simulation parameters for the 1D chain and different power-law exponents σ . L is the system size, N_{sa} is the number of disorder realizations, τ_{eq} is the number of equilibration sweeps, T_{min} is the lowest temperature and N_r the number temperatures used in the exchange Monte Carlo method.

σ	L			N_{sa}	τ_{eq}	T_{min}	N_r
0.00	0.75	0.85	32	4 000	10 000	0.20	20
0.00	0.75	0.85	64	4 000	10 000	0.20	20
0.00	0.75	0.85	128	4 000	10 000	0.20	20
0.00	0.75	0.85	256	4 000	65 000	0.20	20
0.00	0.75		512	2 000	200 000	0.20	20
		0.85	512	2 000	650 000	0.20	20
0.00			1024	1 000	32 000	0.40	26

The model has a very rich phase diagram when the exponent σ is tuned [16]: Both the universality class and the range of the interactions of the model can be continuously tuned by changing the power-law exponent. For $\sigma \leq 1/2$ the model exhibits infinite-range behaviour and corresponds to the SK model. For $1/2 < \sigma \leq 2/3$ we have mean-field behaviour with an effective space dimension $d_{\text{eff}} \geq 6$, whereas for $2/3 < \sigma \lesssim 1$ we have a long-range spin glass with a finite ordering temperature T_c . Close to $\sigma = 2/3$ $d_{\text{eff}} \approx 2/(2\sigma - 1)$ [4]. For $\sigma \geq 1$ $T_c = 0$. In this work we study the SK model [$\sigma = 0$, $T_c = 1$] to test our analysis protocol, as well as the 1D chain for $\sigma = 0.75$ [$T_c \sim 0.69$] and 0.85 [$T_c \sim 0.49$] [17, 18]; both corresponding to the non-mean-field regime. We choose two values which correspond to different effective space dimensions to be able to discern any trends when the effective dimensionality is reduced.

Numerical details — We generate spin-glass configurations by first equilibrating the system at $T \approx 0.4T_c$ using exchange Monte Carlo [19, 20], i.e., $T = 0.4$ for the SK model, 0.27 for $\sigma = 0.75$ and 0.20 for $\sigma = 0.85$. Once the system is in thermal equilibrium we record states ensuring that these are well separated in the Markov process and thus not correlated by measuring autocorrelation times. In practice, if we equilibrate the system for τ_{eq} Monte Carlo sweeps, we generate for each disorder realization 10^3 states separated by $\tau_{\text{eq}}/10$ Monte Carlo sweeps. We test equilibration by equating the energy of the system to the energy computed from the link overlap. Once the data agree within error bars for at least three logarithmically-spaced bins the system is in thermal equilibrium [17]; see Table I for details.

Analysis details — We use an approach closely related to the one used by Hed *et al.* [11]. $M = 10^3$ equilibrium states at $T \approx 0.4T_c$ —to probe deep within the spin-glass phase—are sorted using the average-linkage agglomerative clustering algorithm [21]: Distances are measured in terms of the hamming distance $d_{\alpha\beta} = (1 - |q_{\alpha\beta}|)$, where $q_{\alpha\beta} = N^{-1} \sum_i S_i^\alpha S_i^\beta$ is the spin overlap between states $\{S^\alpha\}$ and $\{S^\beta\}$. The clustering procedure starts with L clusters containing one state and the two closest

lying clusters are merged. The “distance” between two clusters is the average distance between all pairs of members of the clusters. The procedure is iterated until one large cluster is obtained. The sequence of mergers can be displayed by a tree, referred to as a dendrogram. Furthermore, one can plot the distance matrix $d_{\alpha\beta}$ having ordered the states according to the leaves of the dendrogram. This is shown in Fig. 2 where the matrix elements are encoded in gray scale (black corresponds to zero distance). The complex phase-space structure is clearly visible: The matrix has a block-diagonal form, the blocks again being subdivided in a block-diagonal structure.

To analyze the matrix quantitatively for ultrametricity, we randomly select three states from different branches of the tree (cf. Ref. [11]) and sort the distances: $d_{\text{max}} \geq d_{\text{med}} \geq d_{\text{min}}$. We compute the correlator

$$K = (d_{\text{max}} - d_{\text{med}})/\varrho(d), \quad (2)$$

where $\varrho(d)$ is the width of the distribution of distances. Note that the definition of K in Eq. (2) differs from the definition used in Ref. [11] where the normalization is performed with d_{min} . Our choice ensures that any apparent change of an UM measure is scaled out, which is just caused by a width change of the distance distribution. The definition used in Ref. [11] can *only* tell if there is no ultrametricity, i.e., a random bit string will also show an UM response (which we have verified numerically). The definition in Eq. (2) alleviates this problem: For $T > T_c$ (or a random bit string) there is no UM signature in K , whereas for $T \ll T_c$ we see a clear UM response for the SK model. Thus we are able to discern between “trivial ultrametricity,” which occurs from equilateral triangles at $T > T_c$, and a true UM phase space structure. If the phase space is UM then we expect $d_{\text{max}} = d_{\text{med}}$ for $L \rightarrow \infty$. Thus $P(K) \rightarrow \delta(K = 0)$ for $L \rightarrow \infty$ [22]. We have also verified that $P(K)$ does not show any sign of ultrametricity for Migdal-Kadanoff spin glasses [23] where no ultrametricity phase structure is present by construction.

We also analyze the connected components in phase space (visible in the distance matrices $d_{\alpha\beta}$) by extending the approach of Kelley *et al.* [24]. During the i ’th iteration of the clustering algorithm one encounters $M(i) = M - i$ clusters. Thus the goal is to find the number of clusters which represents the data best corresponding to the highest-level blocks in the ordered $d_{\alpha\beta}$ matrix. To obtain a better resolution at the scale of small distances, we use a logarithmic scale $\tilde{d}_{\alpha\beta} \sim 1 - \log d_{\alpha\beta}$, normalized to values $[0, 1)$ [25]. To measure the component property of the configuration space, we calculate for each cluster $\Gamma = \{\alpha_i\}$ obtained during the algorithm the average distance within the cluster (“spread”) $sp_\Gamma = 2 \sum_{\alpha \neq \beta \in \Gamma} \tilde{d}_{\alpha\beta} / |\Gamma|(|\Gamma| - 1)$. Here $|\Gamma|$ is the number of states in the cluster Γ . Then, for each iteration i , the average spread \overline{sp}_i among the $M(i)$ clusters is calculated. Once the clustering analysis is completed, all M

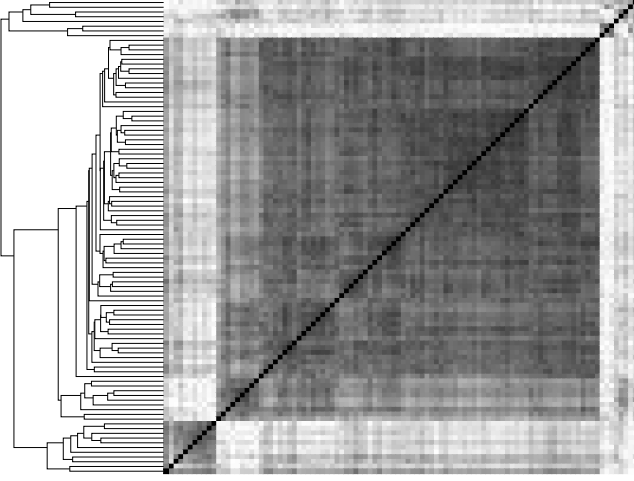


FIG. 2: A dendrogram obtained by clustering 100 configurations (see text) for a sample system with $\sigma = 0.0$ and $L = 512$ at $T = 0.4$ together with the matrix $d_{\alpha\beta}$ shown in grey scale (distance 0 is black). The order of the states is given by the leaves of the dendrogram (figure rotated clockwise by 90°).

average spread values are normalized to lie in the interval $[1, M - 1]$, resulting in $\overline{sp}_i^{\text{norm}}$. For each realization the minimum M_{\min} of $\overline{sp}_i^{\text{norm}} + \gamma M(i)$ as a function of $M(i)$ is determined, where γ is a sensitivity parameter (the method of Ref. [24] corresponds to $\gamma = 1$). Then $n_C = M_{\min}$ is the number of phase-space components. Note that the larger γ is, the fewer components are found. Since a paramagnet should exhibit only one component, we determine for each system size L $\gamma(L)$ such that for $M = 10^3$ random bit strings ($T = \infty$), averaged over 10^2 runs, on average 1.1 components are obtained [26].

Results — In Fig. 3 the distribution $P(K)$ is shown for $\sigma = 0$ (SK model), 0.75 (non-mean-field), 0.85 (non-mean-field) deep in the low-temperature phase ($T \approx 0.4T_c$). In all three cases, $P(K)$ seems to converge to a delta function for $L \rightarrow \infty$. This is clearly visible when looking at the variance of the distribution which decays with a power-law of the system size (Fig. 3 bottom). Note that $P(K)$ does not change with system size close to T_c (inset to Fig. 3, top panel). A similar lack of divergence has also been found for simulations for $\sigma = 4.0$ (not shown). Therefore, the correlator [Eq. (2)] can clearly distinguish between “trivial” ultrametricity—which is due to equilateral triangles—and ultrametricity created by a complex energy landscape.

In Fig. 4 the number of components n_C is shown for $\sigma = 0$ (SK model) as function of systems size for different temperatures T . Below T_c n_C increases with system size, while for larger T it decreases. Other values of σ show a qualitatively similar behavior (not shown). Interestingly, the number of measured components is largest in the spin-glass phase and close to T_c (see inset to Fig. 4). The reason is probably that at higher temperatures more valleys of the energy landscape are accessible, including

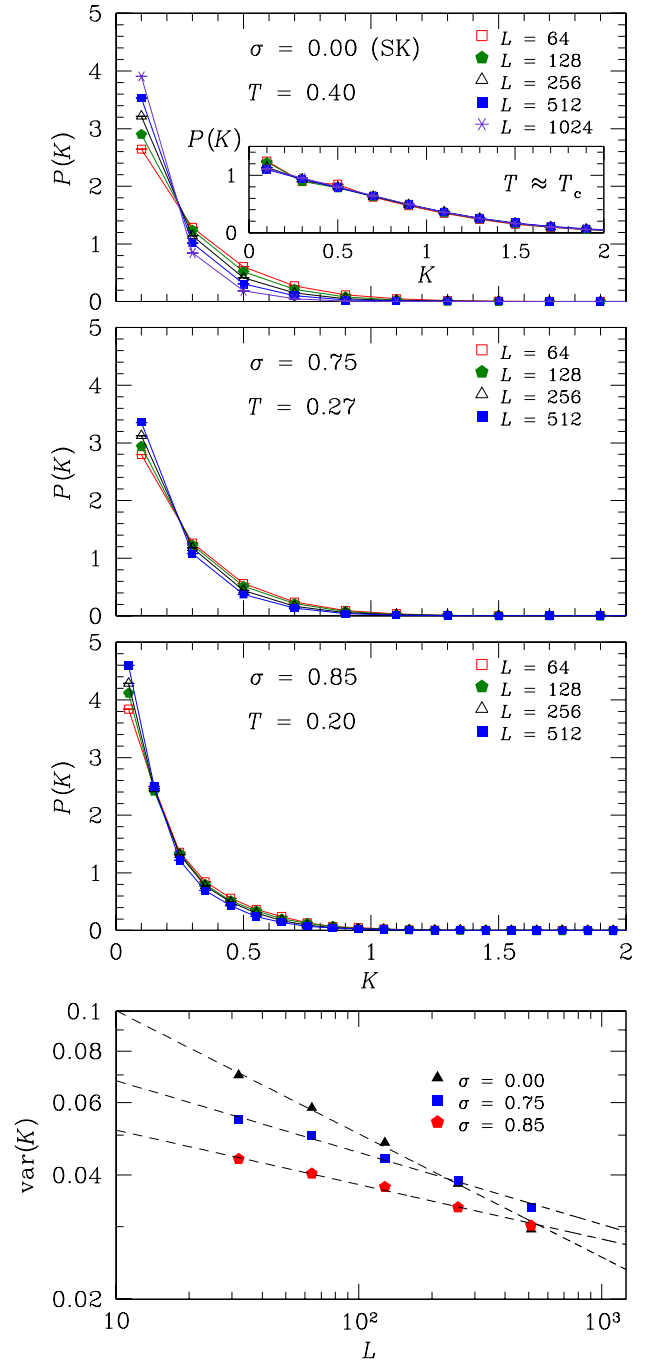


FIG. 3: (Color online) Top set: Distribution $P(K)$ for different system sizes. Top panel: Data for the SK model. The distribution diverges for $K \rightarrow 0$ thus signaling an UM phase structure. Inset: For $T \sim T_c$ no divergence is visible. Middle [bottom] panel: Data for the 1D chain for $\sigma = 0.75$ [0.85] (non-mean-field universality class). The distribution still diverges. Bottom: Variance of $P(K)$ as a function of L for different σ . The data are well fit to a power-law decay $\sim b/L^c$ with $c > 0$ (dashed lines) suggesting a divergence for $K \rightarrow 0$ for all σ . We have also computed the “fraction of UM instances,” (those which exhibit $\int_0^{0.5} P_{\text{instance}}(K) dK \geq 0.5$, not shown). For larger system sizes, this fraction grows with the system size for all σ values. Hence the results for $\sigma > 2/3$ are not due to rare strongly-ultrametric instances.

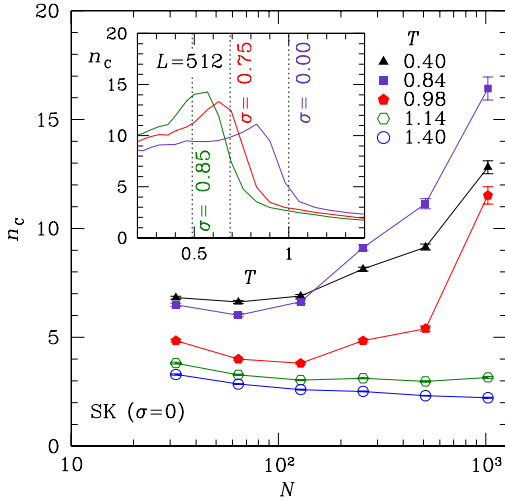


FIG. 4: (Color online) Number of phase-space components n_c in the SK model as a function of system size N for different temperatures. For $T \lesssim T_c$ (full symbols) the number of components grows considerably for increasing system size L , whereas for $T \gtrsim T_c$ (open symbols) the number of components remains approximately constant as a function of L . The inset shows the number of components as a function of temperature T for $L = 512$ for different exponents σ . The data for all σ are qualitatively similar: for $T \sim T_c$ (dotted lines) the number of components is much larger than at $T \gg T_c$.

those who have high-lying minima, still separated by energy barriers rarely overcome. For even higher temperatures even more states are highly populated, leading to basically one big component in the energy landscape. The exact peak position shifts slightly with increasing σ .

Summary and discussion — We have studied numerically the low-temperature configuration landscape of a one-dimensional long-range spin glass with power-law interactions characterized by an exponent σ . By using a hierarchical clustering method and analyzing the resulting distance matrices we have studied the UM properties, as well as counted the components of the phase space. For this purpose we have introduced a novel way to quantify ultrametricity and we have extended a method to count components by analyzing the distance matrix structure. We observe that for values of the power-law exponent σ spanning the infinite-range SK universality class ($\sigma = 0$) to the non-mean-field universality class ($\sigma = 0.75, 0.85$) an UM organization and a complex clustered landscape seem to emerge for the system sizes studied. To see whether these results persist at larger length scales, it would be of interest to study even larger systems. A possible approach would be to study a model with power-law-dependent dilution [27] where even larger system sizes are possible. This is of importance since the system sizes needed to probe the crossover to any putative UM behavior presumably might depend on the system size.

We would like to thank E. Domany, G. Hed, T. Jörg, F. Krzakala and A. P. Young for the useful discussions, as well as T. Jörg for providing test data for the Migdal-Kadanoff spin glasses. We especially thank W. Radenbach for his participation in an initial stage of the project. The simulations have been performed on the Brutus, Gonzales and Hreidar clusters at ETH Zürich. H.G.K. acknowledges support from the Swiss National Science Foundation under Grant No. PP002-114713.

-
- [1] R. Rammal *et al.*, Rev. Mod. Phys. **58**, 765 (1986).
 - [2] G. Parisi, Phys. Rev. Lett. **43**, 1754 (1979).
 - [3] M. Mézard *et al.*, Phys. Rev. Lett. **52**, 1156 (1984).
 - [4] K. Binder and A. P. Young, Rev. Mod. Phys. **58**, 801 (1986).
 - [5] D. Sherrington and S. Kirkpatrick, Phys. Rev. Lett. **35**, 1792 (1975).
 - [6] M. Mézard, G. Parisi, and M. A. Virasoro, *Spin Glass Theory and Beyond* (World Scientific, Singapore, 1987).
 - [7] A. J. Bray and M. A. Moore, in *Heidelberg Colloquium on Glassy Dynamics and Optimization*, edited by L. Van Hemmen and I. Morgenstern (Springer, New York, 1986), p. 121.
 - [8] D. S. Fisher and D. A. Huse, Phys. Rev. Lett. **56**, 1601 (1986).
 - [9] F. Krzakala and O. C. Martin, Phys. Rev. Lett. **85**, 3013 (2000).
 - [10] M. Palassini and A. P. Young, Phys. Rev. Lett. **85**, 3017 (2000).
 - [11] G. Hed, A. P. Young, and E. Domany, Phys. Rev. Lett. **92**, 157201 (2004).
 - [12] S. Franz and F. Ricci-Tersenghi, Phys. Rev. E **61**, 1121 (2000).
 - [13] P. Contucci, C. Giardinà, C. Giberti, G. Parisi, and C. Vernia, Phys. Rev. Lett. **100**, 159702 (2008).
 - [14] T. Jörg and F. Krzakala, Phys. Rev. Lett. **100**, 159701 (2008).
 - [15] G. Kotliar *et al.*, Phys. Rev. B **27**, R602 (1983).
 - [16] H. G. Katzgraber and A. P. Young, Phys. Rev. B **67**, 134410 (2003).
 - [17] H. G. Katzgraber and A. P. Young, Phys. Rev. B **72**, 184416 (2005).
 - [18] L. Leuzzi, J. Phys. A **32**, 1417 (1999).
 - [19] C. Geyer, in *23rd Symposium on the Interface* (1991), p. 156.
 - [20] K. Hukushima and K. Nemoto, J. Phys. Soc. Jpn. **65**, 1604 (1996).
 - [21] A. K. Jain and R. C. Dubes, *Algorithms for Clustering Data* (Prentice-Hall, Englewood Cliffs, USA, 1988).
 - [22] Note that for the definition of K in Ref. [11] $P(K) \rightarrow \delta(0)$ for $L \rightarrow \infty$ also when the system is trivially ultrametric.
 - [23] Data provided by T. Jörg.
 - [24] L. A. Kelley *et al.*, Prot. Engin. **9**, 1063 (1996).
 - [25] The value $d_{\alpha\beta} = 1$, i.e., two equal configurations, does occur with exponentially-small probability for large systems but was never observed.
 - [26] If one required an average value of exactly 1 cluster, the sensitivity would depend on the number of samples.
 - [27] L. Leuzzi *et al.* (2008), (arxiv:cond-mat/0801.4855).